Journal of Chemical and Petroleum Engineering (JChPE)

Print ISSN: 2423-673X Online ISSN: 2423-6721

Experimental Study of Low Speed Impact Test on the Fiber-Metal Composite Toughened with NBR Elastomer

Davoud Hashemabadi, Amir Kaveh*, Mahdi Jafari, Mahmoud Razavizadeh, Mahdi Yarmohammad Tooski

1. Department of Mechanical Engineering, South Tehran Branch, Islamic Azad University, Tehran, Iran. E-mail: d.hashemabadi@yahoo.com
2. Polymer Engineering Department, Amirkabir University of Technology, Tehran, Iran. E-mail: amir_kaveh62@yahoo.com
3. Department of Aerospace engineering, Malek Ashtar University of Technology, Tehran, Iran. E-mail: m.jafari.h@mut.ac.ir
4. Faculty of Materials and Manufacturing engineering, Malek Ashtar University of Technology, Tehran, Iran. E-mail: razavi_75@yahoo.com
5. Department of Mechanical Engineering, South Tehran Branch, Islamic Azad University, Tehran, Iran. E-mail: yarmohammadtoosk@yahoo.com

ARTICLE INFO

Article History:
Received: 01 July 2021
Revised: 11 August 2021
Accepted: 14 August 2021

Article type: Research

Keywords:
FML
Hybrid Composite,
Impact Energy,
Low Velocity Impact,
NBR Elastomer

ABSTRACT

In this experimental study, low velocity impact test with different energy levels was performed on a fiber-metal (FML) structure reinforced with NBR elastomer. The FML structure consisted of a 2024 layer of aluminum as the core, two layers of NBR elastomer on both sides of the aluminum, and a composite layer after the NBR layers, which were made by hand layup method. The composite layers were made of bi-direction carbon fiber fabric as well as phenolic resin. Also, the knocker was made from very high hardness and hit the FML sample with various energy levels (50, 58, and 66 joules). Thus, the present paper studied the effect of different composite thicknesses on the front and back of the core against the three impact energies. One of the notable innovations in this work is the use of NBR elastomer, which acts as a reinforcement in withstanding impact loads. Based on the obtained results, the maximum and minimum amount of contact force absorbed energy, deformation, and contact time was related to P ... 2.2 and P … 1.1 samples. By comparing the P … 2.1 and P… 1.2 samples after the impact test, it was shown that P… 2.1 samples had a softer behavior.

Introduction

Loss of weighting of structures by improving mechanical properties and other properties is particularly important in the transportation industry, such as the automotive, aerospace, and shipbuilding industries [1-5]. Lightweight structures with fleeter carrying capacity have higher speed capability and lower fuel consumption. For this reason, the growth in the use of sandwich materials structures as new materials have received remarkable attention in recent years. Increasing demand for lighter vehicles has led the transportation industry to replace and build different structures than ever before. Meanwhile, the vacuum of familiarity with the mechanical

* Corresponding Author: A. Kaveh (E-mail address: p90132910@aut.ac.ir)

Journal of Chemical and Petroleum Engineering, 2021, 55(2): 319-337.
Publisher: University of Tehran, College of Engineering DOI: 10.22059/jchpe.2021.326492.1354

behavior and strength of some new advanced materials has become clear. The growth in the use of sandwich structures requires sufficient knowledge of all aspects of the difference between these structures and common materials. Consequently, to overcome this problem, further studies in the field of understanding the mechanical behavior of sandwich structures are required. In addition, understanding the impact phenomena and dealing with vehicles in land, air, and sea at low speeds is critical that in the meantime, it seems necessary to know the behaviour of sandwich structures due to their high energy absorption capacity [6-7]. Impact on the fuselage can include low-velocity shocks such as falling loads on the fuselage, collisions with cars and pebbles, and tools falling on the fuselage or bullets hitting the fuselage of warplanes. Any collision that has a speed of less than 10 meters per second falls into this category of collisions [8-11]. Ashna Ghasemi et al. [12] investigated the dynamic response of a high-strength composite metal sheet under impact with small and large objects. According to the obtained results, the use of a thin aluminum sheet between composite layers can improve the impact strength of the sheet. Jaroslaw et al. [13] compared the multilayers behavior of metal-glass fiber-epoxy / aluminum and carbon fiber-epoxy / aluminum. They investigated the effect of fiber orientation as well as analysis of loading time of damage area and depth of destruction and their relationship with different energy levels. The obtained results make it possible to determine the specific points that may occur at certain stages of the degradation process of the multilayer structure. These modes of destruction include local microcracks and delamination, which reduces the stiffness of the multilayer and causes more damage due to cracks in the layer. Also, they found that multilayers containing the carbon fiber were more prone to perforation than multilayers containing the glass fiber and delamination in composites and separation between metal and fiber plates to be the main mode of degradation in metal-fiber multilayers. Moreover, the authors reported that in floret multilayers, the energy absorption is mainly carried out through plastic deformation as well as through delamination and their dispersion. While in coral multilayer (carbon-epoxy/aluminum fibers), the impact energy absorption occurs through penetration and perforation of the multilayer. Metal-fiber multilayers based on thermoplastic composites were investigated by Cantwell et al. [14]. They showed that these multilayers had better impact analysis, energy absorption, and fracture toughness than thermoset matrix multilayers. Boroujerdi et al. [15] conducted an experimental and analytical study of low velocity impact on metal-fiber multilayers. They found that as the initial impact velocity and the resulting impact energy increased, the number of separated layers, the separation area between the broken layers increased. While the energy absorption process of the samples does not change with increasing impact speed. Siddiqui and Dariushi [16] investigated the effect of fiber angle on the absorption energy of low velocity metal-fiber multilayers. They used two sharp impact instruments with energies of 6 and 150 joules. They concluded that the composite layers with zero fiber angles greatly increase the impact resistance of the sample, composite layers with a fiber angle of 90 degrees make the sample more brittle, and composite layers with a fiber angle of 45 degrees increase the absorbed energy if placed on the back of the sample. The applied force causes the composite to break on the 45 degree line, and parallel to the fibers, and this type of failure causes the aluminum layer in front of it to be torn. In other words, the aluminum layer first undergoes a lot of plastic strain and then breaks, which causes a lot of energy to be absorbed by this layer. Ramezani Parsa and Eslami [17] experimentally investigated the effect of amplification of different pre-strains of nitinol memory alloy wires embedded in metal-fiber multilayers against low velocity impact. They used a falling impact instrument to perform their experiments. The studied multilayer material was aluminum-glass-epoxy, in which six wires with pre-strains of 1, 2, and 3% were embedded. The obtained results showed that by increasing the pre-straining of the wires, the duration of the impact of the impact with the part increases, and the shock of the impact force of the impact and the number of

damage decreases. In an experimental study, Torabizadeh [18] analyzed the behavior of sandwich aluminum foam sheets in two types of interconnected procedures and separate procedures against low-speed impact load and their failure shape using computer cross-sectional images. This study indicates that the final destruction and complete failure of aluminum sandwich panels compared to polymer sandwich panels have a smaller range and are healthier than samples after impact, so their mechanical properties and performance will be better after impact. In other studies on foam core sandwich panels, Golestani Pour et al. [19, 20] investigated the amount of energy absorption in foam core sandwich panels. Avila et al. [21] investigated the behavior of composite sheets by impact at low velocities. They investigated the effect of changing the volume percentage of nano clay on the amount of contact force at different levels of impact energy. They reported that the samples with a 5% volume fraction of nano clay show the best performance compared to contact force damping. Ji-Fan et al. [22] investigated the low-velocity impact response in fiber-metal multilayer composites and simple composites. According to the obtained results, the fiber-metal multilayer composites have higher perforation resistance than simple composites. Goo et al. [23] numerically investigated fiber-metal, coral, and glare multilayer composites under low impact velocity. The simulation results for coral show larger critical loads and smaller displacements under the same impact energy. They also investigated the effect of different aluminum alloys on the impact resistance of coral. They showed that by increasing the yield strength of the aluminium alloy, the impact resistance properties are improved. Tsaris et al. [24] studied the impact resistance of fiber-metal multilayer composites under low velocity and then were able to provide an optimal design for the impact resistance of aerospace applications. They also showed that fiber-metal multilayer composites can absorb energy through plastic deformation and fracture between layer interfaces. In particular, delamination has occurred on the back of the aluminum alloy sheet and adjacent to the fiber-reinforced epoxy and between the layers. Ji Fan et al. [25] investigated hole failure in three different layering of fiber-metal multilayer composites under low velocity impact. As reported, increasing the thickness via enhancing the number of layers can increase the impact resistance. Increasing the size of the projectile and the size of the plate leads to an increase in the energy of the perforation and change the location of the projectile impact, has little effect on the impact response in this type of composites. Ning et al. [26] evaluated the improvement of mechanical properties of fiber-metal multilayer composites based on carbon and aluminum reinforced composites by various methods. The test results showed an improvement in mechanical properties through acid etching and the addition of nano materials, which effectively improves the critical load and fracture toughness of the first mode. Zamani et al. [27] investigated the mechanical properties and high impact of polypropylene nanocomposites with multiwalled carbon nanotubes. In this study, the impact strength for the perforated nanocomposite sample is increased to prevent crack propagation. The addition of nano carbons increases the Young's modulus and yield strength of polymer composites. However, the forming ability of the composite has decreased with increasing percentage of multiwalled carbon nanotubes. Liang Zhang et al.[28] studied the influence of viscoelastic parameters, and radius of curvature, on the free and forced vibration characteristics of a model under low-velocity impact. Then, the influence of density of knocker, and weight fraction of the graphene nanoplatelets on the indentation, contact force, absorbed energy in the panel, and indenter velocity was investigated. The obtained results exhibited that the designer, as the weight fraction of the reinforcement increases, the maximum absorbed energy of the GPLRC (Graphene nanoplatelets reinforced composite) panel could happen in less time. Khademzadeh et al. [31] studied the effect of nano-silica and compatibilizer on the morphology, mechanical properties, and linear rheology of the PLA/EVA blends.He found the simultaneous addition of nanoparticles and SEBS-g-MA led to synergistic toughening effects, and the compatibilized blend containing nano-silica exhibited excellent impact toughness.

According to previous studies, the use of NBR rubber and aluminum sheet as the core of fiber-metal composites and their behavior against low-speed impact has not been investigated.

To the best of our knowledge, this is the first report about evaluating the effect of composite layer thickness, impact energy, and the effect of thick and thin composite layers exposed to the impact of the knocker. It is necessary to mention that the composite used in this research was manufactured of carbon fiber fabrics and phenolic resin. Therefore, this study aims to investigate the effect of 50, 55, and 66 joule impacts on a hybrid composite that in the core of it the 2024 aluminum sheet and NBR rubber have been used, and the back and top of the core, carbon fiber-resin composite in different thicknesses, have been used. Consequently, in the present study, the effect of the different thicknesses of the composite on the front and back of the core on the three impact energies has been investigated, and stunning results have been reported.

Experimental

Materials

In this research, fiber-metal multilayer samples, including two composite surfaces and the core consisting of aluminum sheet and NBR rubber, were formed. The aluminum used in the core was made of Al 2024-T3 with a thickness of 0.5 mm. Proper surface preparation of aluminum sheets was inevitable to ensure the adhesive strength of the composite layers to the metal.

Table 1. Mechanical properties of Aluminium 2024-T3

Tensile strength (MPa)	Yield strength (MPa)	Elongation at break (%)
434-441	289	10-15

NBR rubber was glued to the top and bottom of the aluminum sheet. Table 2 presents the properties of the used NBR rubber, respectively.

Table 2. Mechanical properties of NBR

Tensile strength (MPa)	Yield strength (MPa)	Hardening temperature	Elongation at break (%)
67.8	10.5	-200c	150-400

In order to make the composite layers that are placed on both sides of the hybrid composite material, a woven carbon fabric (Torayca T300 carbon fiber) weighing 200 grams per unit area was used. Also, the phenolic resin under the brand name IL800 (Resol type IL800 with red color and manufactured by Rositan Company) was used.

Drop Weight Impact Test

In order to determine the fracture energy of metals and composite materials, a gravity or drop weight testing device has been used. The ASTM D2444 standard was applied for this type of test. This device detects the impact phenomenon not through pre-and post-impact energy, but by giving information during the impact time. In this device, the impact load is applied by dropping a weight whose weight can be changed. The device has barriers that allow the user to adjust the height of the fall, so it is easy to determine the fall's initial energy and apply it to the sample. In order to perform this test, a low speed impact device was used, which was in accordance with the impact test standard. Also, the data recorded by the dynamometer sensor installed on the impact (including a 2.7 kg head made of hardened steel) was transferred to the computer. A data collection device was used to deliver the force-time curve to the user on time. To test, the samples were placed between two plates, then, by closing the four clamps that

connected to the device body, the samples were fixed between the two mentioned plates and were prepared for the test and were hit. The knocker was connected to a plate by two locks, which opened the locks to test, and released the knocker. Fig. 1 shows the gravity impact device.

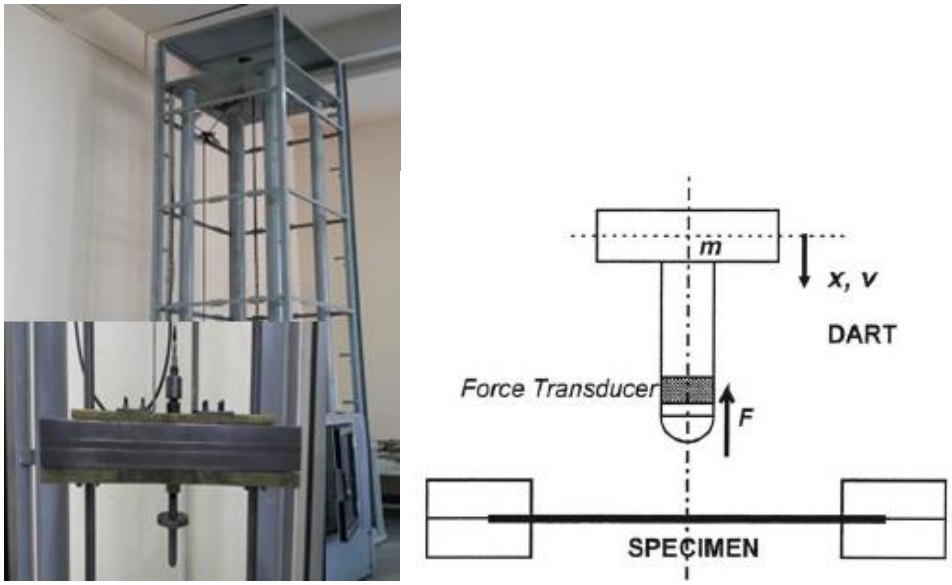

Fig. 1. Setup of Impact test

Manufacturing of Fiber-Metal Multilayers

The hand layup method was used to make of fiber-metal multilayer. Various methods have been proposed to prepare the aluminum surface for adhesive bonding. In this study, to prepare the surfaces of the plates, the sandblasting method was used to prepare and degrease the plates. Fig. 2 shows the prepared aluminum plate.

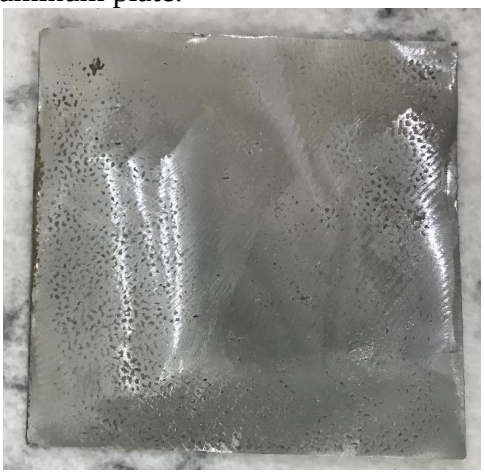

Fig. 2. The surface of aluminum after sandblasting process

In this research, due to the use of NBR and the necessary requirements, the hand layup method has been used. In addition, in order to reinforce the effect between metal and composite and also the high adhesion of the NBR to the composite surface, the NBR elastomer was used. First, carbon fiber fabrics were cut in 15 x 15 cm dimensions. Then the aluminum plates prepared from the previous stage, which have dimensions of 15 * 15 cm, were sanded and prepared. And after ensuring that there was no oxidation on the aluminum primer and chemosile adhesive with codes 211 and 222, it was applied on the aluminum surface with a brush. After one hour of drying and ensuring the adhesion condition, the NBR was glued to the aluminum sheet. After the NBR was bonded, the air trapped between the metal and rubber layers was evacuated with a roller. This bonding was done so that the ratio of 65% of fabric and 35% of resin was observed in the layers.

Fig. 3. Phenolic resin and woven carbon fiber

Then the prepared sample was placed in a hot press with a pressure of 5 tons, and the defined curing cycle for the above-mentioned resin was carried out along with the application of pressure. It should be noted that by placing the element with central heating capability and raising the temperature to 135 °C, the stress in layers increases, which leads to increasing of stiffness factor and impact resistance. Fig. 4 shows some made samples.

Fig. 4. Prepared samples for impact test

Samples and test conditions

In this study, four samples of hybrid composites with different thicknesses were made according to Fig. 5 and were subjected to impact tests with energies of 50, 58, and 66 joules. It should be noted that in this study, three levels of energy were obtained from a fixed mass that was released from different heights.

Table 3. Sequence and thickness of each layer

Sample code	Thickness of Top composite layer(mm)	Thickness of bottom composite layer(mm)	Thickness of Top NBR layer(mm)	Thickness of bottom NBR layer(mm)	Thickness of Al layer(mm)
P..1/1	1	1	0.5	0.5	0.5
P..1/2	1	2	0.5	0.5	0.5
P..2/1	2	1	0.5	0.5	0.5
P..2/2	2	2	0.5	0.5	0.5

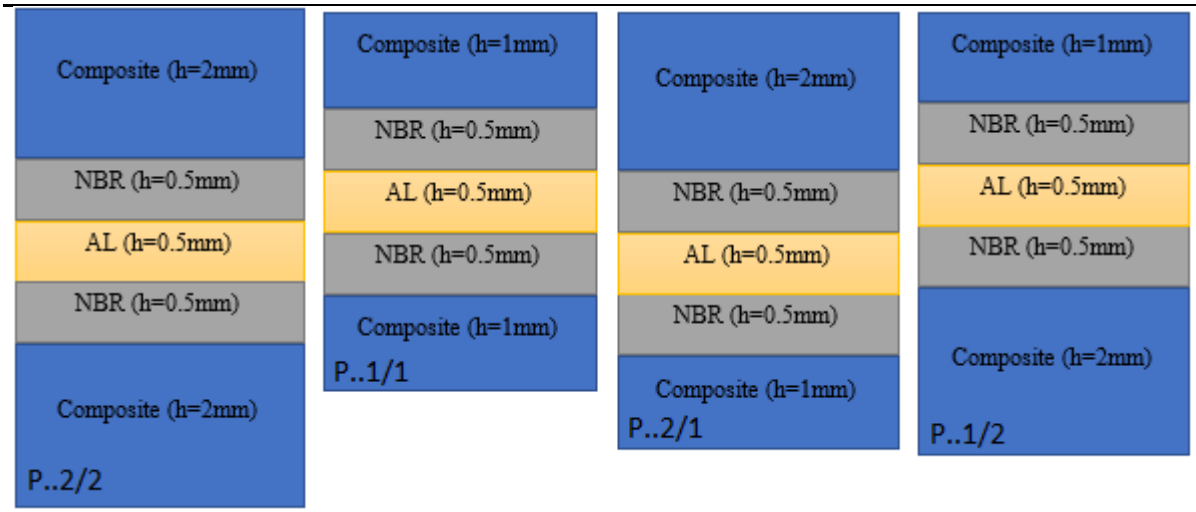

Fig. 5. Schematic of the prepared samples

Another factor that has been studied in this project was impact energy. In this research, all four types of samples shown in Fig. 5 were tested under three impact energies. Therefore, according to the explanations provided in Table 3, the test samples have been coded.

Table 4. Coding of samples under impact test

Codes	Energy (J)	Composite Thickness (mm)
P501/1	50	1 mm top layer and 1 mm bottom layer
P502/2	50	2 mm top layer and 2 mm bottom layer
P502/1	50	2 mm top layer and 1 mm bottom layer
P501/2	50	1 mm top layer and 2 mm bottom layer
P581/1	58	1mm top layer and 1 mm bottom layer
P582/2	58	2 mm top layer and 2 mm bottom layer
P582/1	58	2 mm top layer and 1 mm bottom layer
P581/2	58	1 mm top layer and 2 mm bottom layer
P661/1	66	1 mm top layer and 1 mm bottom layer
P662/2	66	2 mm top layer and 1 mm bottom layer
P662/1	66	2 mm top layer and 1 mm bottom layer
P661/2	66	1 mm top layer and 2 mm bottom layer

According to Table 3, the meaning of the back layer was the side of the hybrid composite that does not strike with the knocker. The top layer also referred to the part of the specimen that the knocker strikes during the test. It is noteworthy that the samples of low speed impact test were prepared according to the standard in the dimensions of 20 * 20 cm. All tests (Table 3) were performed by a hemispherical knocker and its accessories (accelerometer sensor, bearing, etc.) with a mass of 2.7 kg, which strikes the samples from three different heights. Impact velocity and height were obtained using Eqs. 1 and 2 to achieve three energy levels of 50, 58, and 66 joules [29].

$$E = mgh \quad (1)$$

$$V = \sqrt{2gh} \quad (2)$$

In Eqs. 1 and 2, E is the impact energy, m, the impact mass, g is the gravitational acceleration, h is the fall height, and V is the impact velocity. When the knocker strikes the specimens, the acceleration data over time is recorded by a sensor mounted on the knocker and transmitted to the computer via a controller. According to the test results, disturbing signals were observed at the output. By using the averaging method, a curve was passed through the response outputs to reduce the disturbing signals. In addition, suitable low-pass filters were used to eliminate the high frequency signal. After this, Using Eq. 3, the acceleration-time data were converted to force-time data. [29].

$$F(t) = ma(t) \tag{3}$$

In Eq. 3, $F(t)$ is the contact force at each moment of the test, m is the impact mass, and $a(t)$ is the striking acceleration at each moment of the test. After recording the contact force data in terms of time, Using Eq. 4, the velocity data in terms of time were obtained [29].

$$V(t) = V_0 - \int a(t)\, dt \tag{4}$$

In Eq. 4, V(t), the strike velocity, V_0, the strike velocity before the strike, and $a(t)$, is the momentary acceleration. After recording the velocity /time data, if the knocker penetration into the fiber-metal multilayer is neglected, knocker displacement can be equated to the fiber-metal multilayer displacement, which is calculated from Eq. 5 [29].

$$\delta(t) = \int V(t)dt \tag{5}$$

In Eq. 5, $V(t)$ is the strike velocity, and $\delta(t)$ is the knocker displacement. By recording velocity data in terms of displacement, the absorbed energy is calculated using Eq. 6 [30].

$$E = \int F\delta(t)dt \tag{6}$$

Eq. 6, E is the absorbed energy, F is the contact force, and $\delta(t)$ is the knocker displacement. To extract the above data, coding in MATLAB software has been used. Also, after extracting the above data, the damage to the samples has been investigated experimentally.

Results and discussion

As stated in the previous sections, the number of samples examined in this study is 12 samples, and three replications have been done for each sample.
In this section, force-time, force-displacement, energy-force and maximum force diagrams are presented for the following three modes:

- Four samples of impact hybrid composites with the energy of 50 joule
- Four samples of impact hybrid composites with the energy of 58 joule
- Four samples of impact hybrid composites with the energy of 66 joule

In the results section, in order to investigate the failure mechanism in these samples, fracture mapping of the optimum samples was drawn.

Effect of 50 –Joule Impact on the Studied Composite

After performing P501/1, P502/2, P501/2, P502/1 samples, the curves of force-time, force-energy, and displacement force diagrams for 50 joules were presented. Fig. 6 shows the time force diagram for the above four tests.

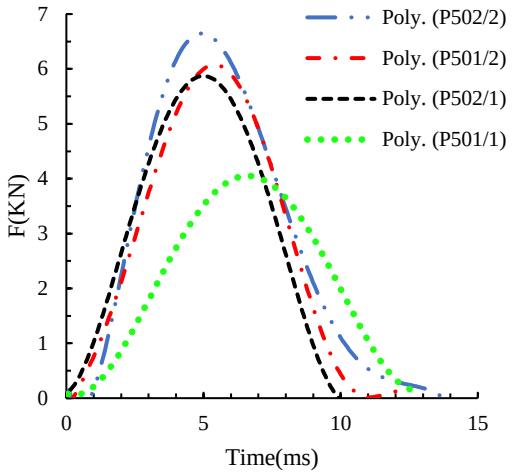

Fig. 6. Force-time diagram for a 50-joule impact

Examining the force-time diagram for the 50 joule test, it can be concluded that the maximum contact time belongs to the P502/2 sample, which means that the P502/2 sample has a softer behavior than the other three samples. Also, according to Fig. 6, P502/1 and P501/2 samples have less contact time than P502/2 and P501/1, which indicates the relative brittleness of these samples. The reason for this can be attributed to the asymmetric thickness of the composite in samples P502/1 and P501/2. According to this Fig. 6, the maximum contact force of the sample is P502/2, which is due to its greater thickness. By comparing the maximum force in P502/1 and P501/2 samples, a slight difference is observed, so the displacement of thick and thin composite layers at 50 joules impact has a greater effect on the contact time.
Fig. 7 shows the four examples of force-displacement diagrams for the 50- joule impact.

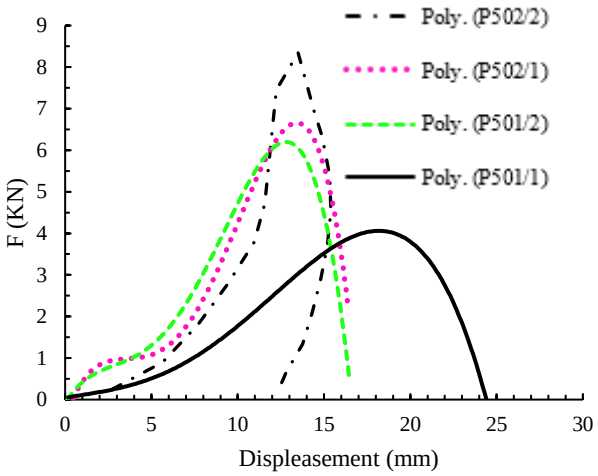

Fig. 7. Force-displacement diagrams for a 50 -joule impact

With examining Fig. 7, it is clear that the maximum force and minimum displacement at the moment of the maximum load have been borne by the P502/2 samples. From this perspective, the best behavior under 50 joules impact was shown by P502/2 sample. According to Fig. 7, the maximum displacement for the P501 sample was about 25 mm. Therefore, this sample is more tolerant of deformation.

In the following, power-energy diagrams and maximum absorbed energy were studied. Fig. 8 shows the energy-force diagram for the above four samples.

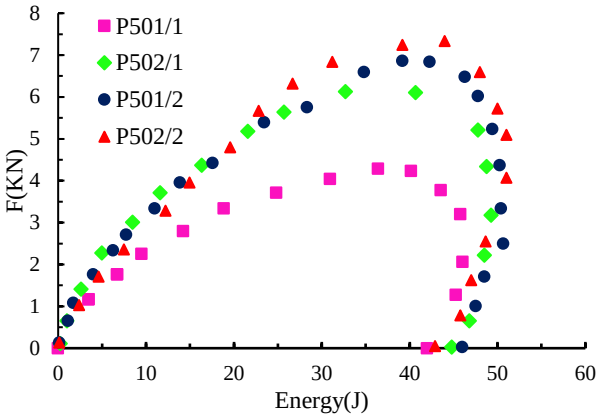

Fig. 8. Power-energy diagram for the 50 -joule impact

According to Fig. 8, the area under the diagrams for sample P502/2 is larger than the rest. As known, strain, and energy, and force have a direct relationship with stress. Just as the area below the strain-stress diagram represented toughness, the area below the energy-force diagram also represented stiffness. According to the explanation, it can be said that the toughness of the P502/2 sample has the highest, and the P501/1 sample has the lowest toughness. It should be noted that the toughness of P501 / 2 is higher than P502, and both of these samples are less than P502/2.

Fig. 9 shows the maximum energy absorbed in all four samples P501/1, P502/2, P501/2, P502/1.

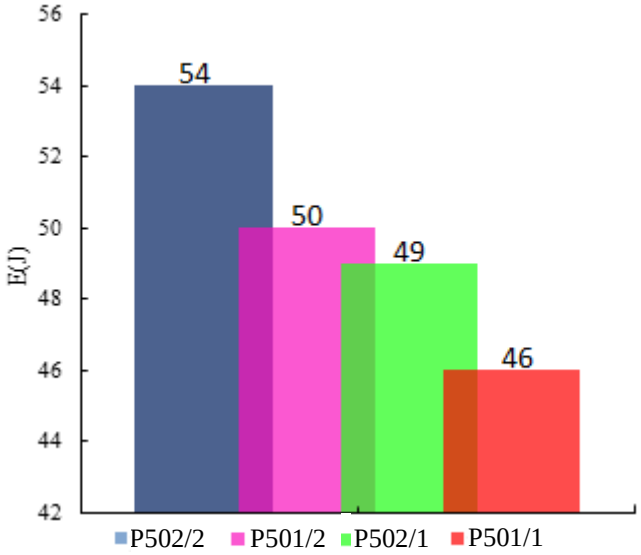

Fig. 9. The Maximum of absorbed energy in P501/1, P502/2, P501/2, P502/1

According to Fig. 9, the maximum energy for the sample is 2.502, and the minimum for P501 is 1.1. Therefore, increasing the thickness of the composite increases the amount of energy absorption.

Effect of 58 –Joule Impact on the Studied Composite

The force-time, force-energy, and force-displacement diagrams obtained from the impact device were studied. First, samples P581 / 1.5, P581 / 2.5, P582 / 1.5, and P582/2 were tested

with an energy level of 58 joules. Because acceleration was recorded over a long period of time, as well as the effect of vibration, the parts that are not part of the impact process must be refined from the impact curve. The results showed the obtained acceleration-time diagram has lots of dispersion. To extract force-time diagrams, it was necessary that the acceleration-time diagram needs to be continuous. For this purpose, the MATLAB software and the Violet command curve were refined and continuous.

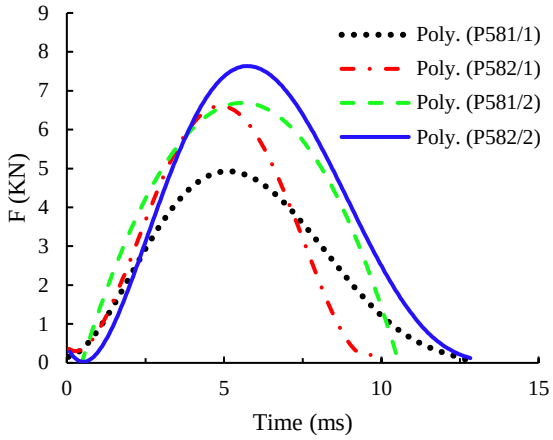

Fig. 10. Force-time diagram for 58- joules impact

As can be seen, P582/2 and P581/1 have higher contact times (between the sample and the colliding body). It is also noticeable that in P582/1, the contact time is much lower than in other samples. It should be noted that due to asymmetric geometry, P581/2.5 and P582/1 have much shorter contact times than P581/1. Also, due to the lower thickness of P581/1, this sample has a much lower maximum force than other samples.

A comparison of the force-displacement diagram for the four samples at 58 joules was given in Fig. 11. As can be seen, the sample P582 / 2 has a higher maximum force than others (between the specimen and the colliding body). As can be seen, the P581/1 has a much lower maximum force than other specimens.

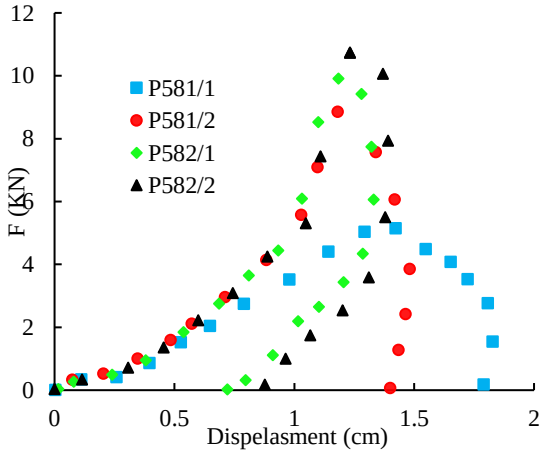

Fig. 11. Force-displacement diagram for 58- joule impact

As shown in Fig. 11, the highest displacement is related to P581/1, and the lowest displacement is related to P582/2 and P582/1. Therefore, although P582/2 and P582/1 samples withstood more force, less displacement occurred in them. And this indicated that in these two samples, the deformation speed was high.

Fig. 12 shows the force-energy diagram for four samples under the 58 joule impact.

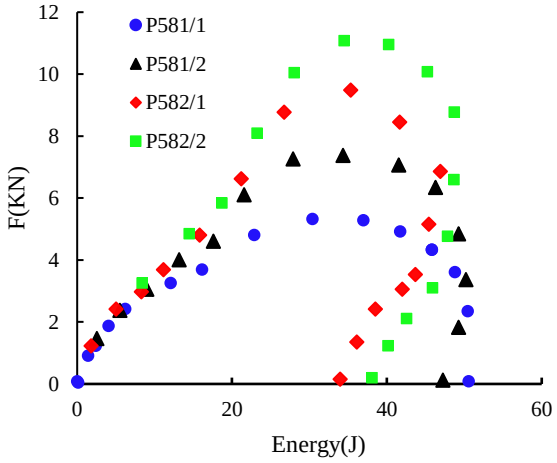

Fig. 12. Force-energy diagram for 58- joule impact

According to Fig. 12, the area under the curve for sample P502/2 was larger than the rest.

Effect of 66- Joules Impact on the Studied Composites

Fig. 13 shows the effect of a 66 joule impact on the force-time diagram of four samples, P661/1, P661/2, P662/1, and P662/2.

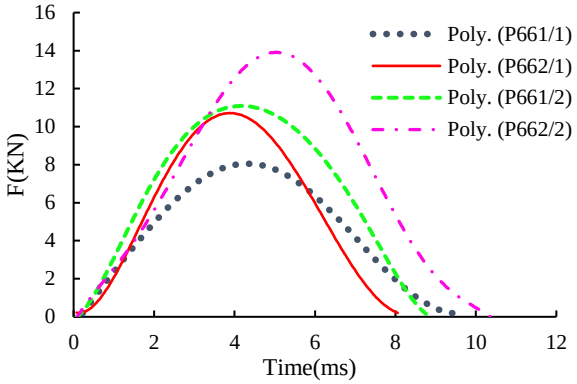

Fig. 13. Force-time diagram for 66- joule impact

According to Fig. 13, by comparing the force-time diagrams, it can be easily seen that the P662/2 sample with a 2 mm composite layer on both sides has the maximum contact force and the maximum contact time. This means that in the 66 joule impact test, the P662/2 has a higher impact resistance. Another noteworthy point in Fig. 13 is that the maximum contact force for the P661/2 and P662/1 samples differs from each other. However, the maximum contact time in P661/2 sample was about 20% longer than P662/1 sample, which was showed a significant difference and this indicated the softer behavior of sample P661/2 than the sample P662/.

Also, as shown in Fig. 13, the maximum contact time for P661/2 and P662/1 samples is shorter than for P661/1 samples.

And the reason for this attractive result was the non-uniform thickness of the composite in the top and outer layer. In other words, the non-uniform thickness of the composite in the surface and outer layer was a kind of defect.

In the following this section, force-displacement diagrams for four samples under the impact of 66 joules were examined. Fig. 14 shows the energy-force diagram at 66 joules for the four samples P661/1, P661/2, P662/1, and P662/2.

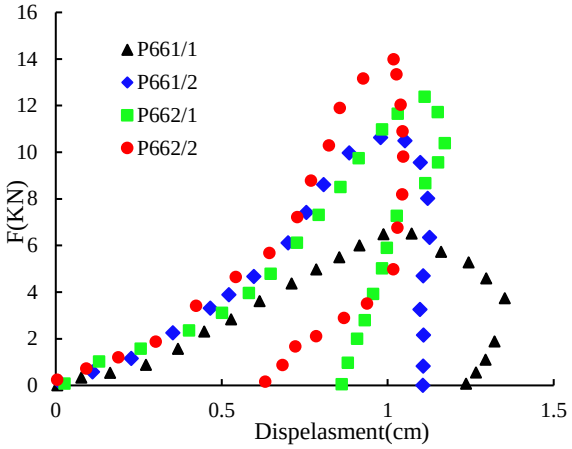

Fig. 14. Force-displacement diagram for 66 –joule impact

According to Fig. 14, the maximum force and the minimum displacement at the moment of maximum force are in the P662/2 sample. Carefully in this Fig, due to the fact that the above three samples were more resistant than the P661/1 sample, it was clear that the slope of the force increasing in the samples P661/2, P662/1, and P662/2 compared to the sample P661/1 was very steep,. Although the P661/1 model had less resistance and less force tolerance but had more displacement at the moment of maximum load, which indicated the soft behavior of this sample.

Fig. 15 shows the force-energy diagram for four samples under the 66 joule impact.

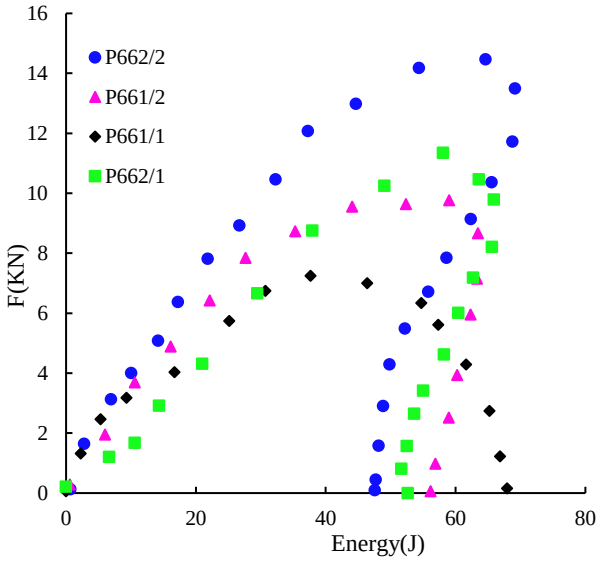

Fig. 15. Energy-displacement diagram for 66 –joule impact

According to Fig. 15, the area under the diagrams for sample P662 / 2 is larger than other samples. As known, strain, and energy have a direct relationship, and force has such a relationship with stress. Just as the area below the strain stress diagram represented toughness, so the area below the energy-force diagram also represents stiffness. According to the presented explanation, it can be said that the toughness of P662/2 has the highest, and P661/1 has the lowest. It should be noted that the toughness of P662/1 is less than P661/1 and both of these samples are less than P662/2. According to Fig. 15, the area below the force-energy diagram in the P662/1 and P661/2 samples is slightly different, which is an attractive result in terms of 66 joules for this hybrid composite. According to Fig. 15, at the moment when the contact force was zero, the P662/2 sample had the lowest energy, and the highest energy in these conditions belonged to the P661/1 sample. This indicated that the P662/2 sample absorbed more energy than the impact test knocker. In other words, the P662/2 had the ability to absorb more energy.

Investigation of Samples after the Tests

To investigate the damage and degradation in hybrid composite samples that have been subjected to impact tests, the samples were examined in terms of appearance. The samples of the tests were divided into four groups of three and were visually examined. Also, by comparing the samples after the test, can be realized the accuracy of the results.
Therefore, in Fig. 16, samples of P502/2, P582/2, and P662/2 after the impact test are presented.

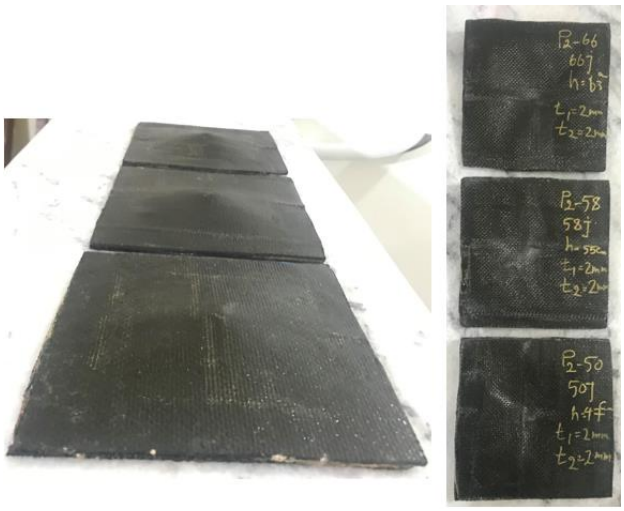

Fig. 16. P502/2, P582/2 and P662/2 samples after impact test

According to Fig. 16, failure did not occur in samples with a composite thickness of 2 mm on both sides. This indicates sufficient resistance of these samples to all three impact energies. According to Fig. 16, it can be seen that the damage caused to the corrosive impact surface in the samples was a type of depression that its amount in the P502/2 sample was less than other samples.
Fig. 17 shows P501/1, P581/1, and P661/1 samples after the impact test.

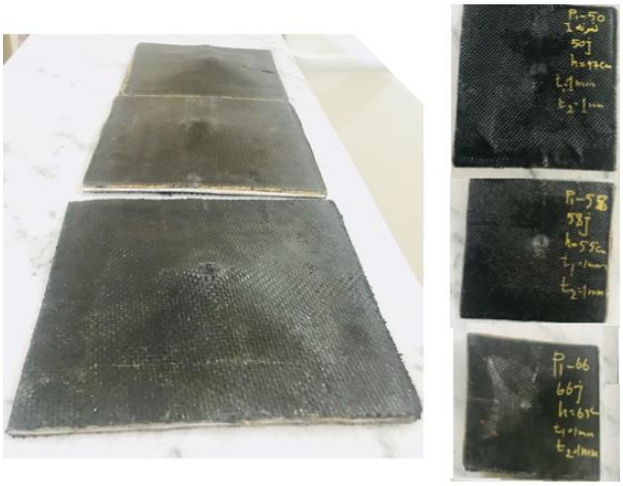

Fig. 17. P501 / 1, P581 / 1 and P661 / 1 samples after impact test

According to Fig. 17, in specimens with a composite thickness of 1 mm on both sides, failure occurred in specimens subjected to 66 joule impact, but the samples that were hit at 50 and 58 Joules did not fail. Therefore, for specimens with a composite thickness of 1 mm on both sides, the maximum impact energy was 58 joules. In other words, the resistance limit of these sheets has been up to 58 joules of impact energy.
Fig. 18 shows P502/1, P582/1 and P662/1 samples after impact test.

Fig. 18. P502 / 1, P582 / 1 and P662 / 1 samples after impact test

According to Fig. 18, in specimens with a composite thickness of 2 mm on the top and 1 mm on the bottom, failure occurred in specimens subjected to 58 and 66 joules, but in specimens subjected to 50 joules, the fracture not occurred. Therefore, for samples with a composite thickness of 2 mm on the top and 1 mm on the bottom, the maximum impact energy was 50 joules. In other words, the resistance limit of these sheets is up to 50 joules of impact energy. By observing the image on the right in Fig. 18 with a little more precision and more sensitivity, it can be said that under all three impacts of 50, 58, and 66 joules, the samples have been damaged. And in the 58 and 66 impacts, the test bullet tore the sample, but in the 50 impacts, only one side of the sample has been torn.

Fig. 19 shows P501/2, P581/2, and P661/2 samples after the impact test.

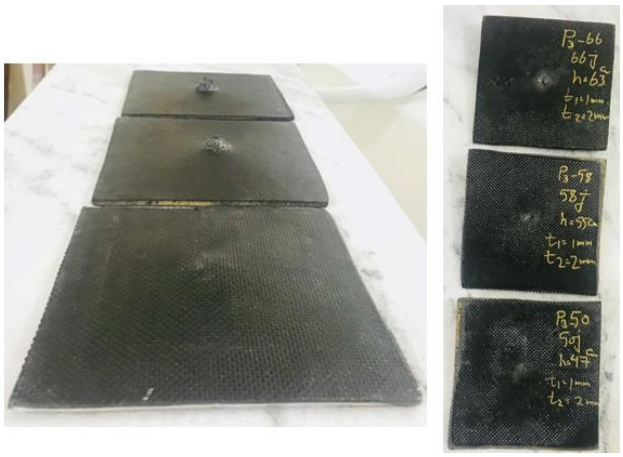

Fig. 19. P501/2, P581/2 and P661/2 samples after impact test

According to Fig. 19, the failure occurred in samples subjected to 58 and 66 joules, but failure did not occur in samples subjected to 50 joules. Therefore, for samples with a composite thickness of 1 mm on the top and 2 mm on the bottom, the maximum impact energy was 50 joules. In other words, the resistance limit of these sheets has been up to 50 joules of impact energy.

By comparing Figs. 18 and 19that presented in Fig. 20, an attractive result was obtained.

Fig. 20. Comparison of P501/2, P581/2 and P661/2 samples with P502/1, P582/1 and P662/ samples after impact test

According to Fig. 20, specimens with a top layer of 1 mm (type A specimens) had undergone more deformation. In other words, type A samples showed the softer behavior. The fact that type A specimens behaved softer means that they have had a longer contact time than Type B specimens. According to the force-time diagrams that were presented in detail in the previous sections, it was observed that the maximum contact time in type B samples was longer than type A samples, which confirmed the soft behavior in type B samples. By observing Fig. 20 with a little more precision and sensitivity, it can be said that type A specimens have been damaged under all three impacts of 50, 58, and 66 joules. However, in type B specimens, the failure occurred in 58 and 66 impacts. In other words, Type B specimens have behaved better against impact load.

Conclusion

Initially, in this research, four types of five-layer hybrid composites were made. Type 1: The middle layer of aluminum and NBR on both sides was placed, and then the carbon-resin fiber composite with a thickness of 2 mm was placed on both sides of the aluminum-NBR structure. Type 2: The middle layer of aluminum and NBR was placed on both sides, and then the carbon-resin fiber composite with a thickness of 1 mm was placed on both sides of the aluminum-NBR structure. Type 3: The middle layer of aluminum and NBR were placed on both sides. Then, the carbon-resin fiber composite layers with 2 and 1 mm thickness were placed on the top and bottom of the aluminum-NBR structure, respectively. Type 4: The middle layer of aluminum and NBR were placed on both sides, and then the carbon-resin fiber composite with a thickness of 1 and 2 mm was placed on the top and bottom of the aluminum-NBR structure, respectively. Therefore, fabricated four types of layered composites in this study and were tested with three impact energies of 50, 58, and 66 joules with low speed. In this study, three impact variables of 50, 58, and 66 joules were examined on four samples. Thus, 12 different modes were obtained to examine this research's time-force, displacement-force and force-energy diagrams. The most important results after analysis have been presented below:

- In all three impact energies of 50, 58, and 66 joules, the P… 2.2 samples had maximum contact force, maximum contact time and energy.
- The maximum contact time was in the P in all three impact energies of 50, 58, and 66 joules, the maximum contact time was in the P… 1.1 samples that it was more than P… 2.1 and P… 1.2 samples.

- In all three impact energies of 50, 58, and 66 joules, the maximum contact force in the P… 1.1 samples were less than P… 2.1 and P… 1.2 samples.
- The appearance checking of the samples showed that the P …1.1 samples had a softer behavior than P / 2.1 and P… 1.2 samples.
- In all three impact energies of 50, 58, and 66 joules, the maximum contact force in the P… 1.2 samples were higher than the P / 2.1 samples. But in the case of maximum contact time, the situation was the opposite. Also, after the impact test, the appearance checking of P … 2.1 and P… 1.2 samples showed that the P… 2.1 samples have a softer behavior than others.
- In samples where the thickness of the composite was different on both sides, the damage was more than in other samples.
- In samples where the composite thickness was considered different on both sides, it was better to have a thin layer of the sample to be in contact with the bullet.

Considering the shape of force-time curves and reviewing the documents, it can be said that in the samples under the applied forces, the failure does not occur in the samples or the shear failure mode has been prevailed. Finally, the results showed that in the P…2.2 samples, energy absorption increased about 40%.

Nomenclature

E	Impact energy (J)
m	Impact mass (Kg)
g	Gravitational acceleration (ms^{-2})
h	Fall height (m)
V	Impact velocity (ms^{-1})
F(t)	Contact force at each momen (N)
a(t)	Striking acceleration at each moment (ms^{-2})
V(t)	Strike velocity at each moment (ms^{-1})
V_0	Strike velocity before the strike (ms^{-1})
t	Time (sec)
δ(t)	Knocker displacement (m)

References

[1] Habibi M, Hashemi R, Ghazanfari A, Naghdabadi R, Assempour A. Forming limit diagrams by including the M–K model in finite element simulation considering the effect of bending. Journal of Materials: Design and Applications. 2018; 230:1-12.

[2] Habibi M, Ghazanfari A, Assempour A, Naghdabadi R, Hashemi R. Determination of Forming Limit Diagram Using Two Modified Finite Element Models. Amirkabir Journal of Mechanical Engineering. 2017; 48:141–144.

[3] Ghazanfari A, Assempuor A, Habibi M, Hashemi R. Investigation on the effective range of the through thickness shear stress on forming limit diagram using modified Marciniak–Kuczynski model. Modares Mechanical Engineering. 2016; 16: 137-143.

[4] Habibi M, Hashemi R, Sadeghi E, Fazaeli A, Ghazanfari A, Lashini H. Enhancing the mechanical properties and formability of low carbon steel with dual-phase microstructures. Journal of Materials Engineering and Performance. 2016; 25: 382-389.

[5] Habibi M, Hashemi R, Tafti MF, Assempour A. Experimental investigation of mechanical properties, formability and forming limit diagrams for tailor-welded blanks produced by friction stir welding. Journal of Manufacturing Processes. 2018; 31: 310-323.

[6] Torabizadeh MA. Response of aluminum foam sandwiches under low velocity impact. Journal of Science and Technology of Composites. 2018; 5:177-184.

[7] Abrate S. Impact on Composite Structures: Cambridge University Press; 2005.

[8] AU A. Prediction of Low-Velocity Impact Damage in Thin Circular Laminates. journal of AIAA. 1985; 23:442-449.
[9] Cantwell W, Morton J. The Impact Resistance of Composite Materials—A Review. Composites. 1991; 22: 347-362.
[10] Richardson M, Wisheart M. Review of Low-Velocity Impact Properties of Composite Materials. Composites Part A: Applied Science and Manufacturing. 1996; 27: 1123-1131.
[11] Sadighi M, Alderliesten R, Benedictus R. Impact Resistance of Fiber-Metal Laminates-A Review. International Journal of Impact Engineering. 2012; 49:77-90.
[12] Ashenai GF, Malekzade FK, Paknejad R. Response of Cantilever Fiber Metal Laminate (FML) Plates Using an Analytical-Numerical Method. Journal of Modares Mechanical Engineering. 2013; 13:57-67.
[13] Jaroslaw B, Barbara S, Patryk J. The Comparison of Low Velocity Impact Resistance of Aluminum/Carbon and Glass Fiber Metal Laminates. Polymer Composites. 2016; 37:1056-1063.
[14] Abdullah M, Cantwell W. The Impact Resistance of Polypropylene-based Fibre–Metal Laminates. Composites Science and Technology. 2006; 66:1682-1693.
[15] Boroujerdy MS, Dariushi S, Sadighi M. Fiber Metal Laminates Under Low Velocity Impact: An Experimental/Analytical Approach. Iranian Journal of Polymer Science and Technology. 2011; 24: 69-78.
[16] Sadighi M, Dariushi S. An Experimental Study on Impact Behavior of Fiber/Metal Laminates. Iranian Journal of Polymer Science and Technology. 2008; 21: 315-327.
[17] Parsa AR, Eslami FR. Influence of Pre Strain Shape Memory Alloy Wire on Impact Properties of Smart Fibers Metal Composite. Journal of Modares Mechanical Engineering. 2017; 17: 322-330.
[18] Torabizadeh MA. Response of aluminum foam sandwiches under low velocity impact, Journal of Science and Technology of Composites. 2018; 5: 177-184.
[19] Golestanipoor M, Babakhani A, Zebarjad M, Tavakoli M, Naderi B. Investigation of Absorbed Energy in Sandwich Panels with Foam-Core under Drilling. Journal of Modern Materials. 2012; 3: 10-15.
[20] Golestanipoor M, Babakhani A, Zebarjad M. Investigation and Simulation of Quasi Static Drilling in Sandwich Panels with FoamCore. Journal of Modern Materials. 2015; 6: 23-28.
[21] Avila AF, Soares MI, Neto AS. A study on nanostructured laminated plates behavior under low-velocity impact loadings. International journal of impact engineering. 2007; 34: 28-41.
[22] Fan J, Cantwell W, Guan Z. The low-velocity impact response of fiber-metal laminates. Journal of Reinforced Plastics and Composites. 2011; 30: 26-35.
[23] Yu GC, Wu LZ, Ma L, Xiong J. Low velocity impact of carbon fiber aluminum laminates. Composite Structures. 2015; 119: 757-766.
[24] Tsartsaris N, Meo M, Dolce F, Polimeno U, Guida M, Marulo F. Low-velocity impact behavior of fiber- metal laminates. Journal of Composite Materials. 2011; 45: 803-814.
[25] Fan J, Guan Z, Cantwell W. Numerical modeling of perforation failure in fibre metal laminates subjected to low velocity impact loading. Composite structures. 2011; 93: 2430-2436.
[26] Ning H, Li Y, Hu N, Arai M, Takizawa N, Liu Y. Experimental and numerical study on the improvement of interlaminar mechanical properties of Al/CFRP laminates. Journal of Materials Processing Technology. 2015; 216: 79-88.
[27] Zamani MM, Fereidoon A, Sabet A. Multi-walled carbon nanotube-filled polypropylene nanocomposites: high velocity impact response and mechanical properties. Iranian Polymer Journal. 2012; 21: 887-894.
[28] Zhanga L, Chenbcde Z, Habibi M. Low-velocity impact, resonance, and frequency responses of FG-GPLRC viscoelastic doubly curved panel. Composite Structures. 2021; 269: 114000.
[29] Ghajar R, Rassaf A. Effect of impactor shape and temperature on the behavior of E-glass/epoxy composite laminates. Modares Mechanical Engineering, 2014; 14:1 -8.
[30] Ramezani PA, Eslami RF. Influence of pre strain shape memory alloy wire on impact properties of smart fibers metal composite. Modares Mechanical Engineering, 2017; 17: 322-330.

[31] Moradi S, KhademzadehYeganeh J. Highly toughened poly(lactic acid) (PLA) prepared through melt blending with ethylene-co-vinyl acetate (EVA) copolymer and simultaneous addition of hydrophilic silica nanoparticles and block copolymer compatibilizer. Polymer Testing, 2020; 91: 106735.

How to cite: Hashemabadi D, Kaveh A, Jafari M, Razavizade M, Yarmohammad-Tooski M. Experimental Study of Low Speed Impact Test on the Fiber-Metal Composite Toughened with NBR Elastomer. Journal of Chemical and Petroleum Engineering. 2021; 55(2): 319-337.